A Numerical Model to Simulate the Time Dependent Behavior of Rock

Kenichi NAKAOKA*, Koji HATA**, Hiroaki KITOH*** and Yujing JIANG****

(Received September 30,2011)

Synopsis

To simulate the time-dependent deformation of the rock, we propose herein a numerical creep model. The model can evaluate consistently from immediately after loading up to collapse considering the confinement effect. In this paper, firstly, a rheological relaxation model consisting of spring and damper components is explained to rock under a constant compressive stress and also under a constant strain rate are simulated using the proposed model. As a result, the obtained time history of strain rate under the constant stress, and also the relation between stress and strain including strain softening behavior under the constant rate are fairly agreed with the test's results.

KEYWORDS: creep, numerical model, strain rate effect, strain-softening

1. Introduction

Under the swelling rock, there is sometimes increasing of ground deformations around the tunnel with time though while the tunnel is not under excavation. And it often make difficulty to continue tunnel excavation, so cause the cost up, and delay the schedule For radioactive waste disposal tunnel, long-term evaluation of deformation is needed for performance assessment because it is concerned that the creep phenomenon continues.

It is known that creep deformation of rock specimen under tri-axial compression test with constant stress-which called "creep test" hereafter, shows three phases of their states. Firstly, strain rate decrease by degrees from fast to slow. Next, the slow strain rate condition continues. Finally, strain rate increase rapidly and collapse. Each of these states is called primary creep, secondary creep, and, tertiary creep, respectively.

By contrast, under tri-axial compression test with constant strain rate, which called "loading test" hereafter, axial stress of specimen decrease beyond its peak stress to residual stress, which is called strain softening.

As the numerical models that can evaluate both the creep deformation and strain softening behavior, there are the elasto-viscoplastic model proposed by Adachi and Oka[1)], and, the model that varies the compliance depending upon time duration and current stress proposed by Okubo and Fukui et al[2)].

For the model by Adachi and Oka[1)], materials parameters have to be modified depend on confined pressure to simulate the tri-axial tests. To make simulation easy, it is desirable to use same parameters through the analysis if the stress changes even in analysis step. Considering the confinement effects easily, Azuma and Ohtsuki et al.[3),4)] modified the Adachi-Oka model by adding the new eight model parameters. While, in Okubo's model, the confinement effect is not considered. Furthermore, for the model, the determination of the model parameters using creep tests results is difficult when evaluation of primary to tertiary creep deformation needed.

In this study, the numerical model introducing a non-dimensional parameter *s* which represents the degree of creep development. The features of the model are easiness of estimating the model parameters because the numbers of parameters are not many. It can evaluate the effect of compression pressure based on Mohr – Coulomb criteria. At first, the numerical model is formulated, and the rheological relaxation model consisting of spring and damper is explained. Next, the model is installed into a finite difference method framework. Then, calculations of creep test and loading test are carried out about the existing tests data using one element model. By comparison between the results of numerical analysis and tri-axial compression test, applicability of the model is discussed.

---

* Student, Doctor Course of Department of Civil Engineering (Obayashi Corporation)

** Obayashi Corporation

*** Associate Professor, Department of Civil Engineering, Osaka City University

**** Professor, Division of System Science, Nagasaki University

2. Creep model

(1) Introduce of non-dimensional parameter *s*

The non- dimensional important parameter *s* indicates the degree of creep development. It is assumed, herein, that the value of *s* increases with repeating of many stop and forward sequences as shown in Fig.1. As shown in the figure, the number of repetition is to be d*s*・*n* within an interval d*s*, so the increment value of *s* with the repetition is 1/*n*. Introducing the stationary time *f* for the stop sequence dependent upon current stress state, moreover, increasing rate of *s* can be described as eq. (1). It is noted that in Fig. 1, the duration for the forward sequences is to be zero, and it for the stop is to be the sum of the time *f*. Strain rate, so called creep strain is proportional to the increasing rate of *s* to be described later in detail.

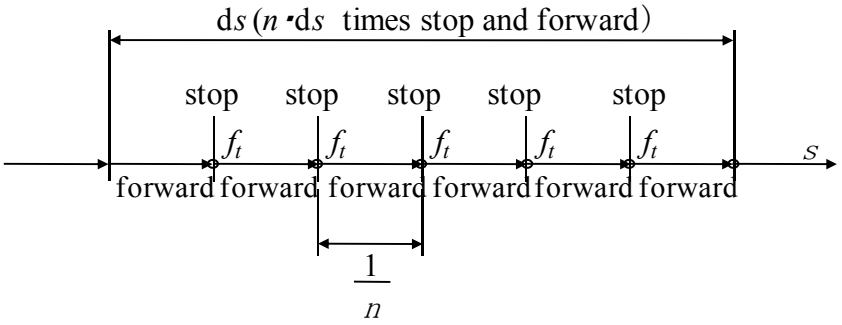

Fig.1 Concept of increasing *s*.

$$\dot{s} = \frac{1}{\mathrm{n}f} \tag{1}$$

The parameter *n* is that means density of the stop sequence duration in unit interval *s*. It is assumed that the parameter *n* varies depending on increments of *s*, and the function of stopping density n=*g*'(*s*) is defined by eq. (2), which is never decrease.

$$n = g'(s) = \frac{\alpha_1}{b_n\sqrt{2\pi}} \exp\left\{-\left(\frac{s-a_v}{\sqrt{2}b_n}\right)^2\right\} \tag{2}$$

Here, b_n and a_v are material constants, these called as variance and mean, respectively, as follows. Parameter α_1 is the maximum value of *g*'(*s*), and π is circular constant. It is assumed, furthermore, that the stationary time *f* is the function of stress *p*, so called *f*'(*p*). Thus, increasing rate of *s* (after, $\dot{s}$) is described by eq. (3) based on eq. (1) and (2). Now, stress *p* is defined as the distance from coordinate of principal stress to hydrostatic axis in three-dimensional principal stress space as shown in Fig.2, which is described as eq. (4). Here, J_2 in eq. (4) is second invariant of deviatoric stress, which is as eq. (5), δ_{ij} in eq. (6) is Kronecker's delta. The increasing concept of *s* is shown in Fig.3 with consideration of stopping density. For creep test's condition, *f*'(*p*) is constant so that every stationary durations of stop sequences is same.

$$\dot{s} = \frac{1}{g'(s)f'(p)} \tag{3}$$

$$p = \sqrt{2J_2} \tag{4}$$

$$J_2 = \frac{1}{2}s_{ij}s_{ij} \tag{5}$$

$$s_{\mathrm{ij}} = \sigma_{ij} - \delta_{ij}\sigma_m \tag{6}$$

$$\sigma_{\mathrm{m}} = \frac{1}{3}\sigma_{ii} \tag{7}$$

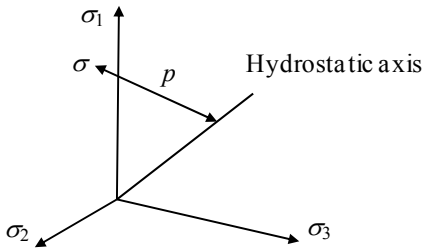

Fig.2 Stress p to increases s.

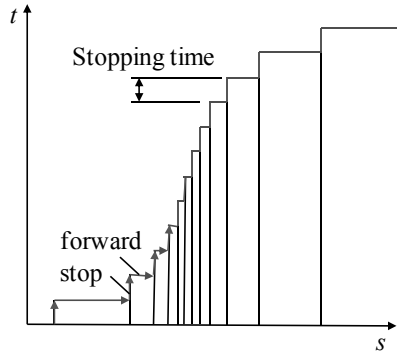

Fig.3 Concept of s increase with consider of stopping density.

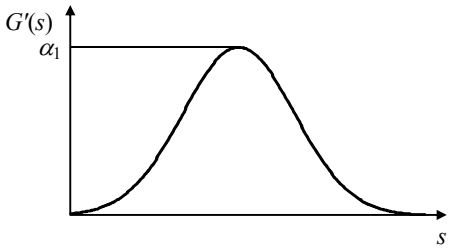

Fig.4 An example of stopping density function.

The concept of this model is based on the assumption as follows: In the case of unconfined material, contact and disconnections will occur between grains, while, in case of rock, the micro cracks will develop and penetrate. At every time of both of the events occurs, the increase of parameter s expressing creep development stops each time. Afterward, the parameter goes forward until next event occurs. For example, at beginning stage of loading under low strain condition, almost grains do not contact each other, or almost micro cracks do not develop so that the number of stopping is small. Subsequently, when the loading stage proceeds, the number increases, because the both events occur evidently. Consequently, approaching at final stage, the number decreases owing to the gradual termination of the both events.

Furthermore, another assumption is introduced here as follows: strain increment with each event is proportional to the deviatoric stress p. It is based on that the event under high stress condition causes considerable large slips or crack extensions, so the strain increment becomes also larger than under low stress condition. Now, consider creep tests, we set parameters $\alpha_1=f_t(p)=1$. $\dot{s}$ curves are obtained as shown in Fig.5 and Fig.7 as numerical solutions for eq. (3). Moreover, the functions of stopping density are as shown in Fig.6 and 8. The s values at $\dot{s}$ minimum in Fig.5 and Fig.7 correspond to the s values at maximum stopping density in Fig.6 and 8.

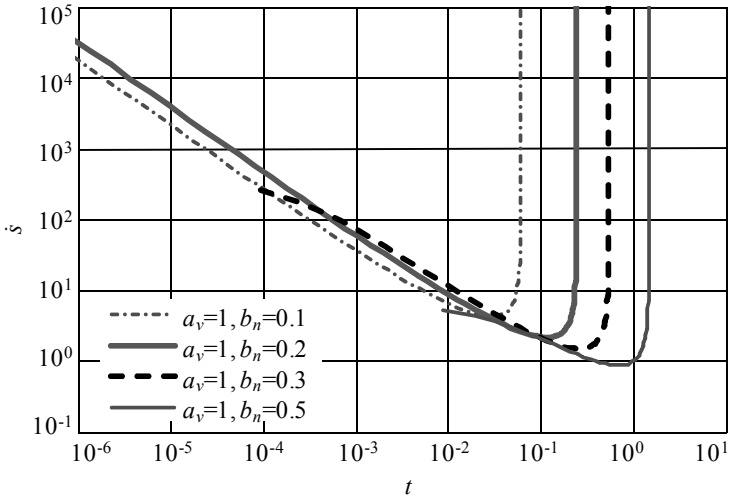

Fig.5 Time history of $\dot{s}$ with various variances: b_n.

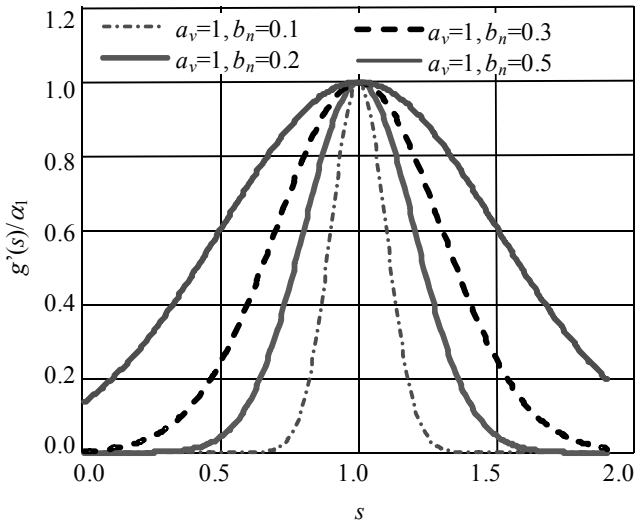

Fig.6 Function of stopping density with various variances: b_n.

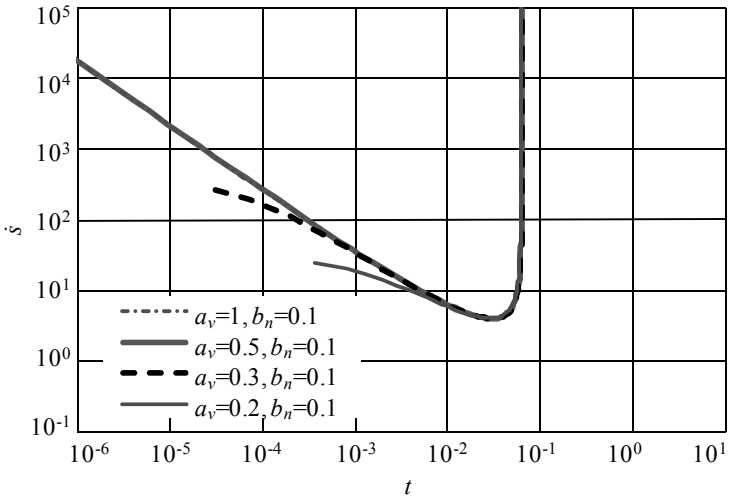

Fig.7 Time history of $\dot{s}$ with various means: a_v.

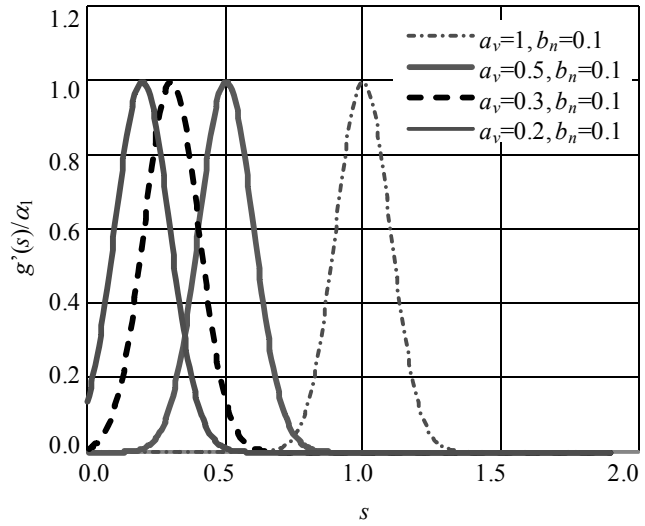

Fig.8 Function of stopping density with various means: a_v.

From these dual logarithmic figures; Figs. 5 and 7, it can be found that, with same mean, the times when $\dot{s}$ is minimum become later with variance increase. While, as the same manner, with same variance, the times when $\dot{s}$ is minimum are similar with variable mean. Inclined straight line lengths before the time of minimum $\dot{s}$ become longer with the mean increase, and become shorter with mean decreasing. Creep strain rate curve calculated by the creep model is similarity shape to Fig.5 or 7. From these figures, the gradient of the length are similar and the value is about 0.9, even though mean and variances are varied. To vary the gradient, parameter n has to be added into stopping density function as eq. (8). With smaller n, the gradient become smaller and curvature near the time when minimum $\dot{s}$ occur become larger. With large n, the gradient become larger and curvature become smaller. The distribution of stopping density is shown by Fig.10.

$$g'(s) = \frac{\alpha_1}{b_n\sqrt{2\pi}} \exp\left\{-\left(\frac{s^n - a_v^n}{\sqrt{2}b_n}\right)^2\right\} \tag{8}$$

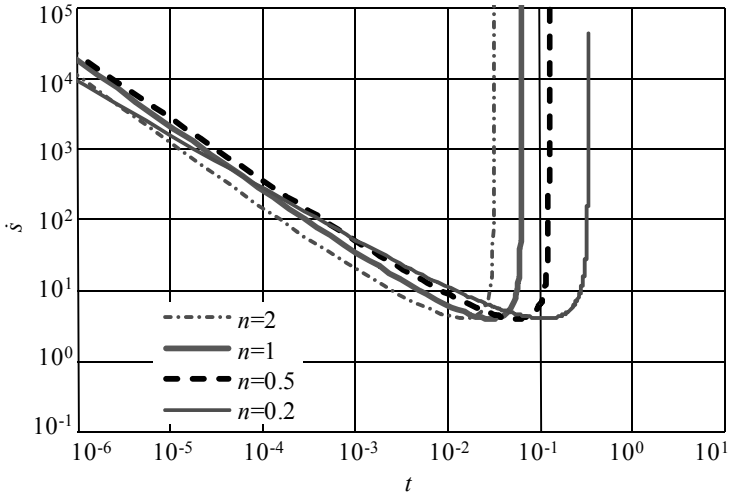

Fig.9 Time history of $\dot{s}$ (variation of n, at a_v=1 and b_n=0.1).

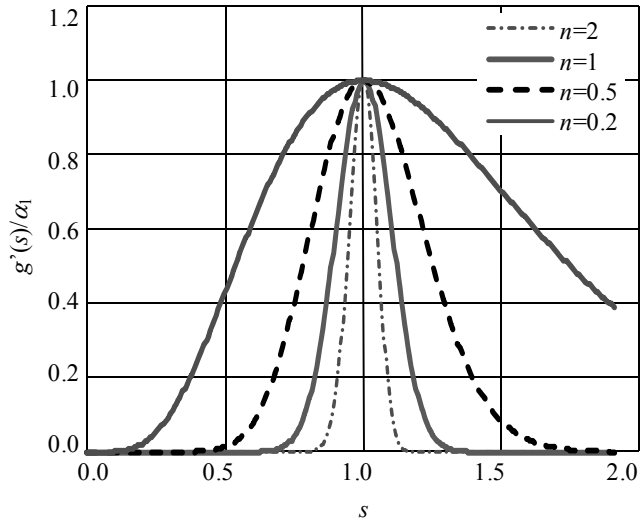

Fig.10 Function of stopping density (variation of n at a_v=1 and b_n=0.1).

Because, many reports about creep tests of rock show that the gradients of straight intervals are near the value 0.9, hereafter, we regard n=1. Next, the function of stopping time is assumed as eq. (9) according to the Arrhenius equation, which rapidly decrease with the intensity of invariant stress p became larger than that of h relevant to shear strength. Parameter h in eq. (9) is obtained from eq. (10) based upon the Mohr-Coulomb criteria.

$$f'(p) = \alpha_2 \exp\{q(h-p)\} \tag{9}$$

$$h = c + \sigma_m \tan\phi \tag{10}$$

Parameters of α_2 and q define the relation between stopping time and p. Furthermore, parameters of c and ϕ define the strength depend on hydrostatic pressure σ_m. By changing of eq. (2) and (9) to eq. (11) and (12), eq. (14) is obtained from eq. (3). The parameter that has to be defined is α in eq. (14).

$$g(s) = \exp\left\{-\left(\frac{s-\mathrm{a_v}}{\sqrt{2}b_n}\right)^2\right\} \tag{11}$$

$$f(p) = \exp\{q(h-p)\} \tag{12}$$

$$\alpha = \frac{b_n\sqrt{2\pi}}{\alpha_1\alpha_2} \tag{13}$$

$$\dot{s} = \frac{\alpha}{g(s)f(p)} \tag{14}$$

(2) Calculation of deviatoric stress p

To install the proposed creep model into a finite difference method framework, FDM, variation of stress due to relaxation is calculated in each loading step previously. By using the stress modifying process additionally, residual force is calculated firstly. Subsequently, after a current incremental stage is convergent, new stress and strain are calculated with the residual force that assumed as load in the FDM. Using obtained residual force, next step to convergence is also done. Finally, next loading step with relaxation calculation is done.

Now, consider a rheological model with spring and damper as shown in Fig.11. The normal force of spring is assumed equal to p shown in Fig.2. It's both ends of the model do not move in process of relaxation calculation. With increments of time step in each loading step, displacement of damper increase and then the force of spring p become smaller. At this process, strain does not change. Next loading step, increment load is added onto spring force, relaxation calculation is repeated again.

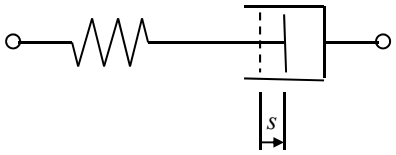

Fig.11 Rheological model

As shown in Fig.11, the displacement of damper is assumed as s indicating degree of the creep development. Being the increment of creep strain by the event of stop and forward sequences as shown in Fig.1 proportional to stress, spring constant is defined as eq. (15). When the spring constant is proportional to stress, relaxation rate becomes faster owing to large stress, and become slower owing to small stress. As the result, the creep strain obtained from convergence calculations satisfies the proportional relation to product of stress p and s. Parameter k' is material constant.

$$k = k'p \tag{15}$$

The flowchart of calculation of relaxation and decreasing of p with time step involved in loading step is shown in Fig.12. The creep strain in Fig.12 is 0.The parameter r in Fig.12 is the stress that increases with creep development to be explained later. It is also assumed that p does not become smaller than r.

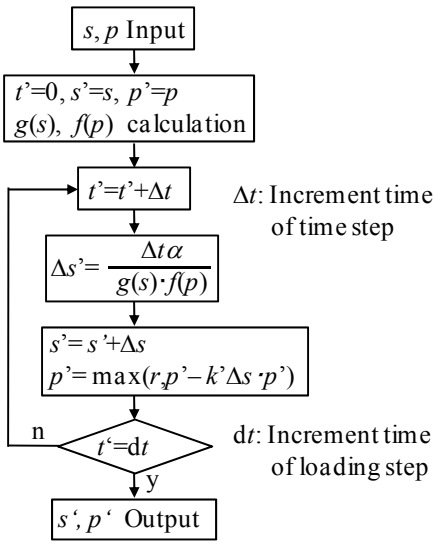

Fig.12 Flowchart of relaxation calculation.

(3) Defining of strength parameter r

The strength parameter r in Fig.12 is to be increases with the accumulated events number as shown in Fig. 1. Thus, r becomes residual strength that is defined by Mohr-Coulomb criteria in eq. (16). Strength parameter r is finally defined by eq. (17).

$$S_r = c_r + \sigma_m \tan(\phi_r) \tag{16}$$

$$r = \frac{S_r}{2}\left\{1 + \mathrm{erf}\,\frac{s - a_v}{\sqrt{2}b_n}\right\} \tag{17}$$

Where, parameters c_r and ϕ_r are cohesion and friction angle at residual stress state, respectively, and σ_m is hydrostatic pressure, erf is error function.

(4) Modifying method of stress using p

Amount of decrease in spring force p is put as dp. Modified spring force is put as p' (= p – dp), and, thus stress calculated from p' is updated as σ_{ij}'. As shown in Fig.13, the direction of stress shift by modifying in

principal stress space is normal according to the well-known von Mises's yield surface. In this case, hydrostatic pressure does not change by modifying of stress. As shown in the figure, at point B, the σ_i is principal stress before modify, point A is hydrostatic pressure σ_m. Point C is principal stress after modifying, and C rides on line A-B. Stress s_i is deviatoric principal stress before modify, $s_i = \sigma_i - \sigma_m$. From figure, deviatoric principal stress after modify s_i' that is described by eq. (18) is same with vector AC. The derivation method of modify the principal stress from point B to C is discussed as follows:

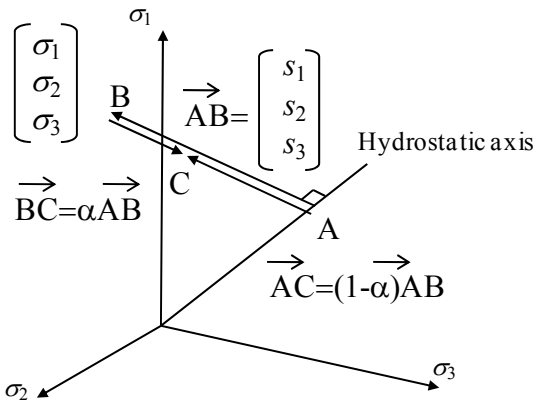

Fig.13 Modify of principal stress

$$s_i' = (1-\alpha)s_i \tag{18}$$

Deviatoric principal stress s_i is defined by eq. (19). Parameter of J_3 is third invariant of deviatoric stress that is defined by eq. (20).

$$s_i^3 - J_2 s_i - J_3 = 0 \tag{19}$$

$$J_3 = \frac{1}{3} s_{ij} s_{jk} \tag{20}$$

Deviatoric stress after modifying is put s_{ij}' as eq. (21).

$$s_{ij}' = (1-\alpha)s_{ij} \tag{21}$$

Second and third stress invariants after modifying of J_2' and J_3' are defined by eq. (22) using invariant stress before modifying.

$$J_2' = \frac{1}{2} s_{ij}' s_{ij}' = \frac{1}{2}(1-\alpha)^2 s_{ij} s_{ij} = (1-\alpha)^2 J_2 \tag{22}$$

$$J_3' = \frac{1}{3} s_{ij}' s_{jk}' s_{ki}' = \frac{1}{3}(1-\alpha)^3 s_{ij} s_{jk} s_{ki} = (1-\alpha)^3 J_3 \tag{23}$$

From eq. (22) and (23), stress invariants before modifying are defined as eq. (24) and (25).

$$J_2 = \frac{J_2'}{(1-\alpha)^2} \tag{24}$$

$$J_3 = \frac{J_3'}{(1-\alpha)^3} \tag{25}$$

By substitution of eq. (24) and (25) into eq. (18) and multiplying by $(1-\alpha)^3$, next equation is obtained.

$$\{(1-\alpha)s_i\}^3 - J_2'(1-\alpha)s_i - J_3' = 0 \tag{26}$$

Comparing with eq. (19) and eq. (26), it is found that the stress s_i' defined in eq. (18) is same as deviatoric

principal stress of deviatoric stress s_{ij} after modifying. So the hydrostatic pressure σ_m' after modifying is equal to hydrostatic pressure σ_m before modifying eq. (27) is given from eq. (21).

$$\sigma'_{ij} - \delta_{ij}\sigma'_m = \sigma'_{ij} - \delta_{ij}\sigma_m = (1-\alpha)(\sigma_{ij} - \delta_{ij}\sigma_m) \tag{27}$$

Stress σ_{ij}' after modifying is given as eq. (28) from eq. (27). Parameter α is given by eq. (29) that is derived from eq. (24).

$$\begin{aligned}
\sigma'_x &= \sigma_x - \alpha\sigma_x + \alpha\sigma_m \\
\sigma'_y &= \sigma_y - \alpha\sigma_y + \alpha\sigma_m \\
\sigma'_z &= \sigma_z - \alpha\sigma_z + \alpha\sigma_m \\
\tau'_{xy} &= (1-\alpha)\tau_{xy} \\
\tau'_{yz} &= (1-\alpha)\tau_{yz} \\
\tau'_{zx} &= (1-\alpha)
\end{aligned} \tag{28}$$

$$\alpha = 1 - \sqrt{\frac{J'_2}{J_2}} \tag{29}$$

If we consider the volumetric creep strain, it is possible to use the elasto-plasticity constitutive equation based on flowing rule. Here, creep strain is assumed as plastic strain ε^p_{ij}. Calculation method of stress modified using constitutive equation is discussed below. Strain inclement in an incremental loading step $d\varepsilon_{ji}$ is given by sum of elastic strain $d\varepsilon^e_{ij}$ and plastic strain $d\varepsilon^p_{ij}$ as shown by eq. (30).

$$d\varepsilon_{\mathrm{ij}} = d\varepsilon^{\mathrm{e}}_{\mathrm{ij}} + d\varepsilon^{\mathrm{p}}_{\mathrm{ij}} \tag{30}$$

Incremental creep strain is defined by eq. (31).

$$d\varepsilon^p_{ij} = H\frac{\partial g}{\partial \sigma_{ij}} \tag{31}$$

Here, function g defines the direction of creep strain in principal stress field. In the case of the direction is normal with the von Mises's yield surface, the function become as eq. (32). Parameter H defines the amplitude of creep strain. In the process in relaxation calculation, total increment strain $d\varepsilon_{ij} = 0$, eq. (33) is obtained from eq. (30) and (31).

$$g = \sqrt{2\mathrm{J}_2} \tag{32}$$

$$\mathrm{d}\varepsilon^e_{ij} = -\mathrm{d}\varepsilon^p_{ij} = -H\frac{\partial g}{\partial \sigma_{ij}} \tag{33}$$

Using the vector of partial differential of $g(\sigma)$ by each stress component, eq. (34) is obtained from eq. (33). After here, vector representation of stress is used.

$$\{\mathrm{d}\varepsilon^e\} = -\frac{H}{\sqrt{2J_2}}\{F\} \tag{34}$$

$$\{F\} = \{\sigma_x - \sigma_m, \sigma_y - \sigma_m, \sigma_z - \sigma_m, 2\tau_{xy}, 2\tau_{yz}, 2\tau_{zx}\}^{\mathrm{T}} \tag{35}$$

Relation of incremental elastic strain and incremental stress is defined with strain-stress matrix D.

$$\{d\sigma\} = D\{d\varepsilon^e\} \tag{36}$$

By putting β as eq. (37), the difference of stress $\{\mathrm{d}\sigma\}$ by modifying is obtained by eq. (38) from eq. (34).

$$\beta = -\frac{\mathrm{H}}{\sqrt{2J_2}} \tag{37}$$

$$\{\mathrm{d}\sigma\} = \beta D\{F\} \tag{38}$$

From eq. (38), by multiplication of D and $\{F\}$, $\{\mathrm{d}\sigma\}$ is obtained as eq. (39). Here, G is the shear elasticity modulus.

$$\{\mathrm{d}\sigma\} = 2G\beta\{\sigma_x - \sigma_m, \sigma_y - \sigma_m, \sigma_z - \sigma_m, \tau_{xy}, \tau_{yz}, \tau_{zx}\}^{\mathrm{T}} \tag{39}$$

Also $\{\mathrm{d}\sigma\}$ is described as eq. (40), the relation σ_m'=σ_m is obtained by solving for stress after modify using eq. (39) and (40). And by solving for deviator stress eq. (41) is derived.

$$\{\mathrm{d}\sigma\} = \{\sigma_x' - \sigma_x, \sigma_y' - \sigma_y, \sigma_z' - \sigma_z, \tau_{xy}' - \tau_{xy}, \tau_{yz}' - \tau_{yz}, \tau_{zx}' - \tau_{zx}\}^{\mathrm{T}} \tag{40}$$

$$\begin{aligned}
\sigma_x' - \sigma_m' &= (1 + 2\mathrm{G}\beta)(\sigma_x - \sigma_m) \\
\sigma_y' - \sigma_m' &= (1 + 2\mathrm{G}\beta)(\sigma_y - \sigma_m) \\
\sigma_z' - \sigma_m' &= (1 + 2\mathrm{G}\beta)(\sigma_z - \sigma_m) \\
\tau_{xy}' &= (1 + 2\mathrm{G}\beta)\tau_{xy} \\
\tau_{yz}' &= (1 + 2\mathrm{G}\beta)\tau_{yz} \\
\tau_{zx}' &= (1 + 2\mathrm{G}\beta)\tau_{zx}
\end{aligned} \tag{41}$$

By square the both side of eq. (41), relation of J_2 and J_2' is obtained as eq. (42). And substitution of β described in eq. (37) into eq. (42) give H as eq. (43).

$$J_2' = (1 + 2\mathrm{G}\beta)^2 J_2 \tag{42}$$

$$H = \frac{\sqrt{2J_2'} - \sqrt{2J_2}}{2G} \tag{43}$$

By substitution of $1 + 2G\beta$ that is described using J_2 and J_2' using eq. (42) into eq. (39), same result of eq. (28) is derived. Volumetric strain with creep deformation becomes zero by solving of the $\mathrm{d}\varepsilon_x + \mathrm{d}\varepsilon_y + \mathrm{d}\varepsilon_z$ using eq. (34) and (35). Evaluation of dilatancy effect enable by giving the gradient of the surface that is defined by g in eq. (32) about hydrostatic axis in principal stress field. Here, direction of creep strain depends on the stress only. Degree of creep s has no relation with the direction.

(5) Method of calculation of creep strain

The strain is evaluated by the calculation that the residual force assumed as load. The residual force is calculated by stress that modified by using decreased p.

3. Simulation of tri-axial confined test

(1) Condition of test and material parameters

The stress modified by the process previously discussed is introduced into the FDM. While, tri-axial confining test with constant axial strain rate so-called loading test and with constant axial load so-called creep test are simulated. Here, one element FDM model is used. Target tests are two[4), 5)] (Case1 and Case2 each). Sedimentary rock is used as specimen for both tests. Each creep tests of Cases1 and 2, such as 70%, 80%, and 90% loads of peak deviator stress resulted from loading tests is applied. Table 1 shows condition of tri-axial compression tests. Table 2 shows model parameters for calculation. Each parameter is adjusted to fit the results of calculation with tests results. Parameters relevant to the time dependence are α, a_v, b_n, k', c, ϕ, q. Herein, α is assumed 1, and b_n is assumed a_v/5 to the straight line length before the time of minimum strain rate in Fig.7 becomes longer. These parameters can be also adjusted separately from residual strength parameters c_r and ϕ_r. It is confirmed by test calculation that Poisson's ratio ν has almost no influence with results. It is assumed ν = 0.3.

Table 1 Conditions of tests.

	unit	Case1[4)]	Case2[5)]
Confine stress σ_c (loading, creep test)	MPa	0.6	0.5
Strain rate (loading test)	%/min	0.1	0.01

Table 2 Material parameters.

	unit	Case1	Case1
E (Young's modulus)	MPa	900	900
ν (Poisson's ratio)	-	0.3	0.3
α (Parameter for increase rate of s, set as 1)	1/min	1	1
a_v (mean)	-	400	200
b_n (variance, set as a_v/5)	-	80	40
k' (spring modulus of rheological model)	-	0.0035	0.01
c (cohesion)	MPa	0.16	0.7
ϕ (friction angle)	drgree	47	47
q (coefficient of sensitivity for stopping time)	1/MPa	22	22
c_r (cohesion of residual stress state)	MPa	0	0
ϕ_r (friction angle of residual stress state)	drgree	51	56

(2) Results

Comparison between calculation and test results of Case1 and Case2 are shown in Fig.14 to 17. From Fig.14 and 16, it is shown that the specific curves of creep rate were simulated satisfactory. The time rapidly strain rate increases, furthermore, were also agreed with that for each case. In Fig.14, the reason of the lines did not continue at tertiary creep is that the overflow of $\dot{s}$ occurred along the iteration for convergence. However, the time of that was considered as frailer time. While, for the loading tests, peak values of each case obtained numerically corresponded well, and strain – stress relations were also fairly agreed. From Fig.18 of the time history of strain, it can be seen the behavior from primary creep to tertiary creep was satisfactory simulated consistently.

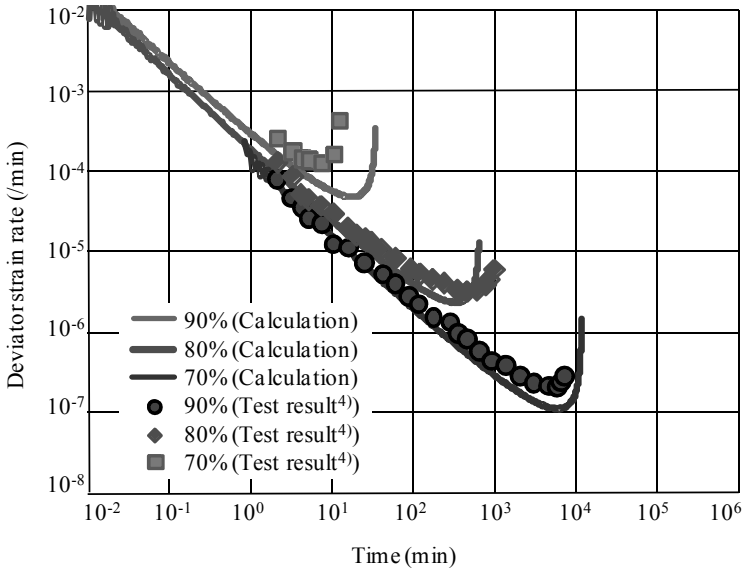

Fig.14 Strain rate by calculation of creep test (Case1, confined pressure σ_c=0.6MPa).

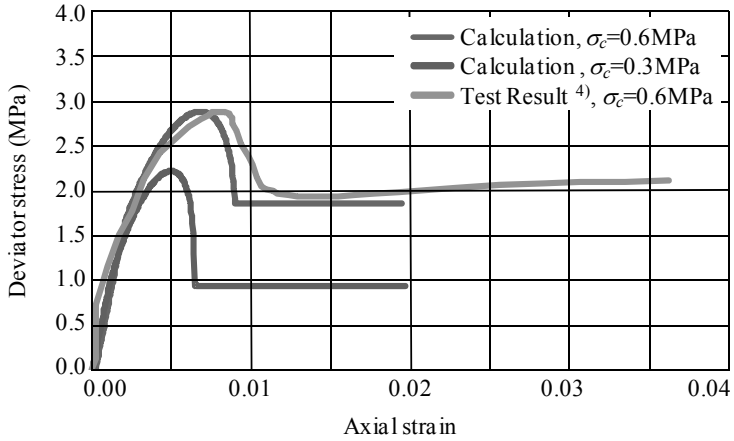

Fig.15 Stress – strain relation by calculation of loading test (Case1, σ_c=0.6、0.3MPa).

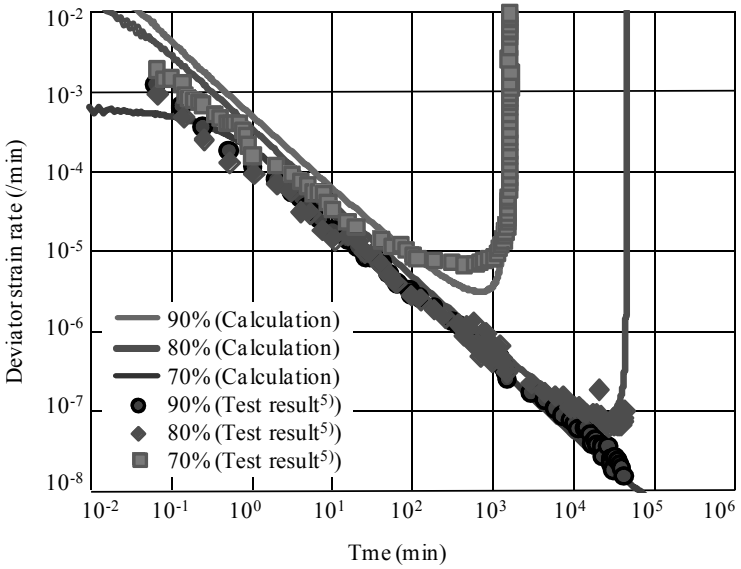

Fig.16 Strain rate by calculation of creep test (Case2, σ_c=0.5MPa).

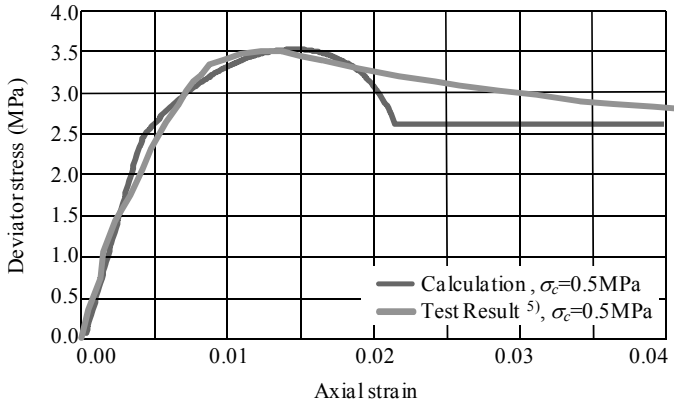

Fig.17 Stress – strain relation by calculation of loading test (Case2, σ_c=0.5MPa).

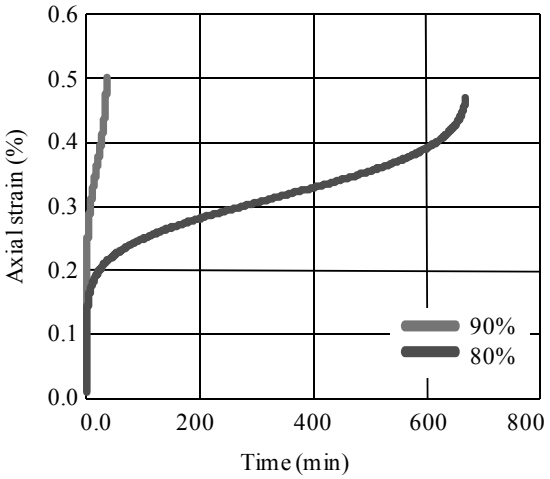

Fig.18 Time history of strain (Case1, σ_c=0.6MPa).

Fig.19 shows the relation between strain rate and peak stress obtained numerically relevant to loading test. The peak stress was lager at the region when strain rate became faster. The relation of peak stress and strain rate in dual logarithm graphs was liner, which was caused by the derivation of this relation in eq. (9). Because it is reported that the peak stress is proportional to logarithm strain rate6) as described by eq. (44), the relation obtained by calculation is identical to eq. (44).

$$p_j = p_0 + a\log\frac{\dot{\varepsilon}}{\dot{\varepsilon}_0} \tag{44}$$

where, p_j is deviator stress, p_0 and $\dot{\varepsilon}_0$ are basis deviator stress and strain rate, respectively, and, a is gradient of line as shown in Fig.19.

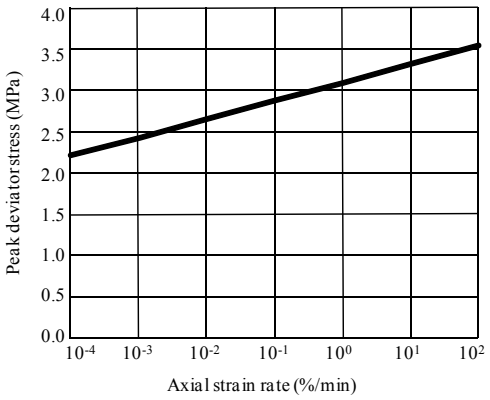

Fig.19 Peak stress vary with strain rate obtained by calculation (Case1, σ_c=0.6MPa).

Fig.20 shows the relation of deviatoric stress and the time obtained numerically when strain rate became the minimum for creep test. The time of minimum strain rate increases exponentially with stress decreasing. The liner relation of stress and logarithms time as shown in Fig.20 is also suitable to eq. (9).

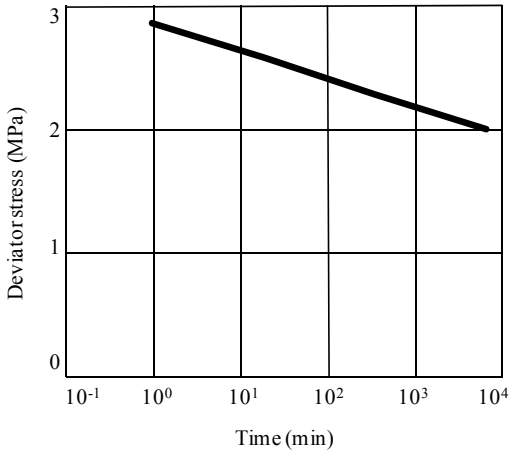

Fig.20 Time at minimum strain rate (Case1, σ_c=0.6MPa).

Fig.21 shows an obtained result on the relation of confined stress and peak stress for loading test. It is shown that the peak stress increase linearly with confined stress, which agree with the Mohr – Coulomb failure criterion. The gradient of the line is dependent upon loading strain rate. For example, when loading rate is very slow, peak stress become equal to residual strength, so the gradient coincide with ϕ_r.

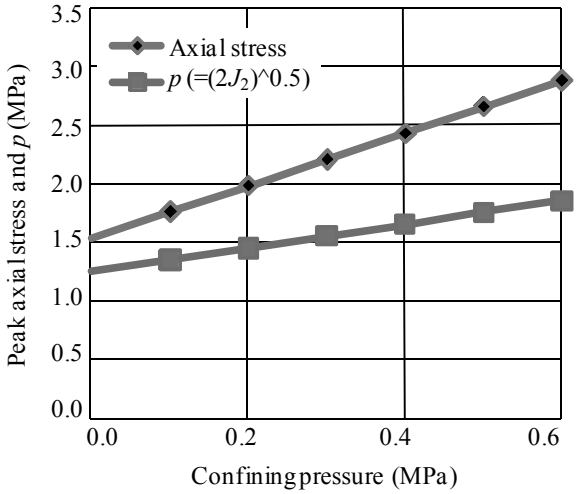

Fig.21 Peak deviator stress vary with confining pressure obtained by calculation (Case1, σ_c=0.6MPa).

4. Conclusion

In this paper, a numerical model to evaluate the creep behavior including strain softening of rock is proposed. The predominant parameter *s* which corresponds to degree of creep development is introduced. To describe the strain rate depend on time or creep strain increase, the function of normal distribution is used as reference. Furthermore, dependence of stress is described by refer to Arrhenius equation. The rheological model consisted of spring and dumper is also developed, which is remarkable that the spring force is equal to deviator stress, to install into the finite difference framework. Numerical simulation for an existing evidence of creep and loading test under the tri-axial confining condition were performed. From creep test simulation, the strain rate curve with primary to tertiary creep was obtained. While, from loading test simulation, stress – strain relation curve with strain softening behavior was also obtained. The both simulation results have a good agreement with test results using same model parameters.

The concern of this model is indicated as follows: The parameter *s* for the rock, under higher stress than residual stress, absolutely increases. Accordingly, parameter *s* becomes higher than a_v and then stress approaches to residual stress under natural conditions. However, many creep tests show the creep behavior from primary to tertiary creep. It follows that the initial *s* of many specimens is lower than a_v. If there is rock that has stress higher than residual strength under natural conditions, it ~~is~~ may be difficult to simulate the

creep behavior of such a rock by using the proposed model herein.

1) Adach, T., Oka, F.: An elasto-viscoplastic constitutive model for frozen sand, Proceedings of the JSCE, no.454(III-20), pp.75-81, 1992. (in Japanese)
2) Okubo, S., Fukui, K., Hashiba, K.: Extension of constitutive equation of variable compliance type and its validation based on uniaxial compression and tension tests of Sanjome Andesite, Shigen – to – Sozai, Vol. 119, pp.541-546, 2003. (in Japanese)
3) Azuma H., Tasaka, Y., Uno, H., Zhang, F, Yasima, A: Improvement of strain softening type elasto-viscouse-plastic model considering confining pressure and strain rate dependency of deformation and strength characteristic, 58th National Science Convention, CS7-056, 2003
4) Nishi, K.: Study on elast-plastic behavior of geological materials and application to design of foundations, CRIEPI report, No. 304, pp. 93, 103, 1982. (in Japanese)
5) Ohtsuki, H., Tasaka, Y., Suzuki, Y., Ohmori, T., Kishida, K., Adachi, T.: Expansion of a soil-water coupled elasto-visco-plastic model and its application to cavern excavation in soft rock, Proceedings of the 35th Symposium on Rock Mechanics, pp.231-236, 2006. (in Japanese)
6) Yong, R. N. and Japp, R. D.: Stress-strain behavior of clays in dynamic compression, vibrational effects of earthquakes on soil and foundations, ASTM, STP, 450, pp.233-262, 1969